Methylation of the p16^{INK4A} promoter is associated with malignant behavior in abdominal extra-adrenal paragangliomas but not pheochromocytomas

N B Kiss[1], J Geli[1,2], F Lundberg[1], C Avci[1], D Velazquez-Fernandez[1], J Hashemi[1], G Weber[3], A Höög[4], T J Ekström[2], M Bäckdahl[1] and C Larsson[1]

[1]Department of Molecular Medicine and Surgery, Karolinska Institutet, Karolinska University Hospital-Solna, CMM L8:01; SE-171 76 Stockholm, Sweden
[2]Department of Clinical Neuroscience, Karolinska Institutet, Karolinska University Hospital-Solna, Stockholm, Sweden
[3]Laboratoire d'Etude des Parasites Génétiques (LEPG), Université François Rabelais, UFR des Sciences et Techniques, Tours, France
[4]Department of Oncology-Pathology, Karolinska Institutet, Karolinska University Hospital-Solna, Stockholm, Sweden

(Correspondence should be addressed to N B Kiss; Email: nimrod.kiss@ki.se)

Abstract

Pheochromocytomas and abdominal extra-adrenal paragangliomas are related to endocrine tumors of the sympathetic nervous system. Studies in animal models have shown that inactivation of the products of the cyclin dependent kinase inhibitor 2A (CDKN2A) gene locus, p16^{INK4A} and p14^{ARF}, promotes the development of pheochromocytoma, especially in malignant form. The present study evaluated the involvement of CDKN2A in human pheochromocytomas and abdominal extra-adrenal paragangliomas from 55 patients. Promoter methylation was assessed using quantitative Pyrosequencing and methylation-specific PCR, and mRNA expression was measured by quantitative real-time PCR. For p16, western blot analysis and sequencing were also performed. succinate dehydrogenase complex subunit B (SDHB) sequencing analysis included extra-adrenal paragangliomas, all tumors classified as malignant, and cases diagnosed at 30 years or younger. The p16^{INK4A} promoter was heavily methylated in a subset of paragangliomas, and this was significantly associated with malignancy ($P<0.0043$) and SDHB mutation ($P<0.002$). p16^{INK4A} mRNA expression showed moderate suppression in malignant cases ($P<0.05$). In contrast, very little p14^{ARF} promoter methylation was seen and there was no significant difference in p14^{ARF} expression between tumors and normal samples. The p16 protein expression was reduced in 16 tumors, and sequence variations were observed in four tumors including the missense mutation A57V and the single nucleotide polymorphism (SNP) A148T. The results suggest that p16^{INK4A}, and not p14^{ARF}, is a subject of frequent involvement in these tumors. Importantly, hypermethylation of the p16^{INK4A} promoter was significantly associated with malignancy and metastasis, and SDHB gene mutations. This finding suggests an etiological link and could provide a clinical utility for diagnostic purposes.

Endocrine-Related Cancer (2008) **15** 609–621

Introduction

Abdominal tumors of the peripheral sympathetic nervous system include pheochromocytomas of the adrenal medulla and extra-adrenal paragangliomas originating from similar chromaffin cells in abdominal sympathetic paraganglia outside the adrenal. The term 'extra-adrenal paraganglioma' also comprises tumors of parasympathetic origin in the head and neck regions that do not secrete catecholamines (WHO classification; Kimura *et al*. 2004, Tischler *et al*. 2004). This tumor type is not included in the present study, which is focused on catecholamine-secreting tumors of the abdomen (in the following referred to as

1351–0088/08/015–609 © 2008 Society for Endocrinology *Printed in Great Britain*
DOI: 10.1677/ERC-07-0285
Online version via http://www.endocrinology-journals.org

'pheochromocytomas' and 'paragangliomas'). These tumors are morphologically and functionally similar, although malignant disease is more common in paraganglioma (Edström-Elder *et al*. 2003). Genetic alterations are generally overlapping between the two tumor types including both somatic alterations and frequent germline mutations in predisposing genes (Edström *et al*. 2000, Nakamura & Kaelin 2006). Pheochromocytomas and paragangliomas may occur sporadically or be part of a heritable disease such as multiple endocrine neoplasia 2A, neurofibromatosis type 1, von Hippel Lindau disease, or familial paraganglioma (Neumann *et al*. 2002, Bryant *et al*. 2003, Elder *et al*. 2005). Mutations in the succinate dehydrogenase complex subunit B (SDHB) gene are prevalent in familial forms associated with malignancy; however, the penetrance for these mutations is moderate (Benn *et al*. 2003, Neumann *et al*. 2004).

Promoter methylation is an important mechanism through which tumor suppressor gene inactivation occurs both in human cancers (Esteller 2003, 2005, Feinberg & Tycko 2004) and transformed cell lines (Antequera *et al*. 1990). Methylation primarily occurs at CpGs, i.e., cytosines located 5′ to guanosines (Holliday & Grigg 1993). The CpG motif is abundant in promoter regions of many genes and methylation is considered to induce the closure of chromatin structures, thereby hindering transcriptional factors from accessing the target DNA stretches (Baylin *et al*. 1998, De Smet *et al*. 1999, McCabe & Caudill 2005).

$p16^{INK4A}$ and $p14^{ARF}$ are two tumor suppressors transcribed from the cyclin dependent kinase inhibitor 2A (CDKN2A) gene locus, which are inactivated in many types of human cancers and transformed cell lines (Baylin *et al*. 1998, Esteller *et al*. 2001, Rocco & Sidransky 2001). p16 and p14 are unrelated proteins that are encoded from the different transcripts and controlled by separate promoter regions (Quelle *et al*. 1995; Fig. 1). Due to alternative splicing, $p16^{INK4A}$ and $p14^{ARF}$ transcripts have distinct first exons (exon 1α and 1β respectively) but share the second and third exons, although in different reading frames (Mao *et al*. 1995, Quelle *et al*. 1995; Fig. 1). p16 and p14 proteins have important functions in cell-cycle regulation (Serrano *et al*. 1993, Sharpless & DePinho 1999) and generally function as negative regulators of cell-cycle progression. $p16^{INK4A}$ acts mainly via the retinoblastoma (RB) pathway by inhibiting the cyclin-dependent kinases CDK4 and CDK6, and $p14^{ARF}$ is important for the p53 pathway as an inhibitor of mouse double minute 2 homologue (MDM2) (Sharpless 2005).

Mice hemizygously deficient for the tumor suppressor gene Pten are particularly prone to develop unilateral pheochromocytomas, thus serving as a model for disease development (You *et al*. 2002). Furthermore in Pten-Ink4a/Arf knockout mouse, bilateral pheochromocytomas developed more rapidly after hemizygous Ink4a/Arf inactivation, and for the homozygous form metastases were also observed (You *et al*. 2002). These findings implicate that the loss of

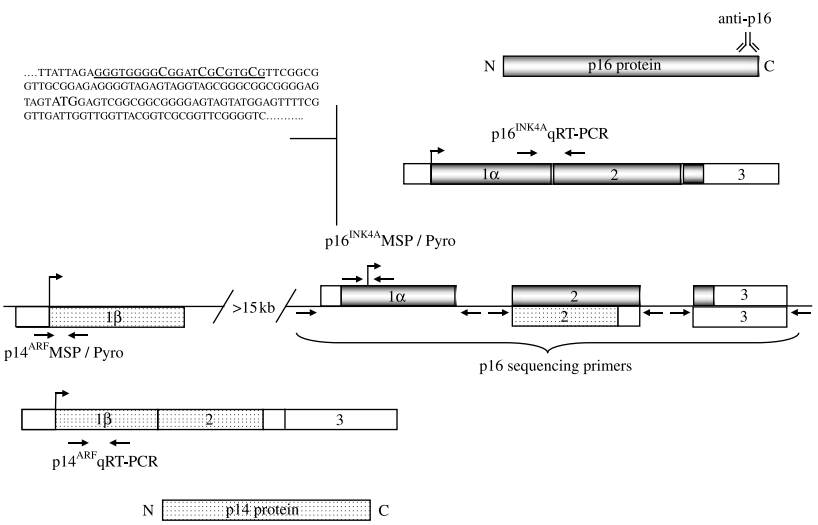

Figure 1 Schematic of the CDKN2A gene locus, the alternate transcripts $p16^{INK4A}$ and $p14^{ARF}$, and their encoded proteins p16 and p14. Horizontal arrows indicate the location of oligonucleotides used for analyses by MSP, qRT-PCR, and sequencing. The individual ATGs are similarly indicated. The location of the antibody used for Western blot is shown at the C-terminal of the p16 protein. The sequence shown at the upper left represents the $p16^{INK4A}$ promoter region sequence after bisulfite treatment of hypermethylated DNA. The placement of the $p16^{INK4A}$ primers used for MSP is indicated in bold, while the sequence detected by Pyrosequencing is underlined. Capital C represents methylation sites identified by Pyrosequencing.

$p16^{INK4A}$ and $p14^{ARF}$ is an important event in the development of this tumor type. In human pheochromocytomas, the loss of heterozygosity at the CDKN2A gene locus in 9p21 has not been observed (Aguiar *et al.* 1996). However, qualitatively assessed $p16^{INK4A}$ promoter methylation was noted in a subset of pheochromocytomas (Dammann *et al.* 2005).

The goal of this study was to investigate pheochromocytomas and paragangliomas for the involvement of $p16^{INK4A}$ and $p14^{ARF}$, a so far less investigated aspect of these tumor types. Promoter methylation was studied by methylation-specific PCR (MSP), as well as by Pyrosequencing, to quantify methylation density. As we observed $p16^{INK4A}$ hypermethylation and mRNA suppression in association with malignant disease, we were prompted to further analyze the $p16^{INK4A}$ sequence and the p16 protein levels.

Materials and methods

Cell lines

SAOS-2 (osteosarcoma) and MCF-7 (breast cancer) were kindly provided by Dr Dan Grandér (Department of Oncology-Pathology, Karolinska Institutet, Stockholm, Sweden) and used as positive and negative controls for p16 expression in western blot assay respectively (Table 1). Cells were cultured in RPMI or Dulbecco's Modified Eagle's Medium (DMEM) at 37 °C in 5% CO_2, with the addition of 8 mM L-glutamine, 1% penicillin/streptomycin (PEST) (5000 U/ml penicillin and 5000 μg/ml streptomycin), and 10% fetal calf serum.

Patients and tumor samples

Fifty-seven samples of pheochromocytomas ($n=44$) or paragangliomas ($n=13$) were obtained from 55 patients who were operated at the Endocrine Surgical Unit of the Karolinska University Hospital, Solna, between 1985 and 2004. These cases have been extensively reviewed and are detailed in previous publications (Edström-Elder *et al.* 2003, Geli *et al.* 2007; Supplementary Table 1, which can be viewed online at http://erc.endocrinology-journals.org/supplemental/). Informed consent was obtained from all patients, and the local ethics committee at the Karolinska University Hospital approved the study of the tissue material.

Fifty-five of the tumors are primary and two are metastases (48Met from 45 and 51Met from 47; Supplementary Table 1). Classification followed the criteria of the US Armed Forces Institute of Pathology (AFIP), whereby extensive local invasion and/or distant metastasis were required to establish malignancy (Lack 1997). The quality of all specimens was verified by histopathological evaluation whereafter samples which contained more than 70% tumor cells were included in the study.

Table 1 Results from analyses of $p16^{INK4A}$ and $p14^{ARF}$ and their expression in normal controls and cell lines

		Analyses of $p16^{INK4A}$				Analyses of $p14^{ARF}$		
				Expression			Pyro CpG 1–13	
Sample no.	Source (+treatment)	MSP	Pyrosequencing CpG 1–4 (%)	mRNA	Western	MSP	Mean (range %)	mRNA
NAP	Whole adrenal pool	n/a	n/a	1.0	n/a	n/a	n/a	1.0
Norm 1	Adrenal medulla	n/a	0/0/0/0	n/a	n/a	Yes	n/a	1.24
Norm 2	Adrenal medulla	n/a	0/0/0/0	n/a	n/a	Yes	n/a	n/a
Norm 3	Adrenal medulla	n/a	0/0/0/0	n/a	n/a	Yes	n/a	1.85
Norm 4	Adrenal medulla	n/a	0/0/0/0	n/a	n/a	Yes	n/a	0.67
Norm 5	Adrenal medulla	n/a	0/0/0/0	2.36	n/a	Yes	n/a	1.16
Norm 6	Adrenal medulla	n/a	0/0/0/0	0.89	n/a	Yes	n/a	0.36
Norm 7	Adrenal medulla	n/a	0/0/0/0	4.44	n/a	Yes	n/a	0.67
Norm 8	Adrenal medulla	n/a	0/0/0/0	0.29	n/a	Yes	n/a	0.63
Norm 9	Whole adrenal	n/a	0/5/0/0	n/a	+	n/a	1.4 (0–2)	1.02
Norm 10	Whole adrenal	No	0/0/0/0	n/a	+	No	2.7 (2–3)	n/a
Norm 11	Lymphocytes	–	–	n/a	n/a	–	–	n/a
Norm 12	Lymphocytes+B	No	0/0/0/0	n/a	n/a	No	1.8 (0–3)	n/a
Norm 13	Lymphocytes+*Sss*1+B	Yes	14/22/26/23	n/a	n/a	Yes	62.5 (52–70)	n/a
MCF-7	Breast cancer cells	n/a	n/a	n/a	+/−	n/a	n/a	n/a
SAOS-2	Osteosarcoma cells	n/a	n/a	n/a	++	n/a	n/a	n/a

n/a, not analyzed or not applicable; +/−, reduced/lost; +, normal range: ++, increased. B, bisulphate treatment; −, no product, as expected.

Non-tumor controls

Detailed information on the normal controls has been published previously (Geli *et al*. 2007; Table 1). Pooled RNA from whole normal adrenal glands of 62 Caucasian subjects (here designated as the normal adrenal pool, NAP) was purchased from Clontech, and RNA and DNA from histopathologically evaluated normal adrenal medulla (Norm 1–8) were acquired from Clinomics Biosciences Inc. (Watervliet, NY, USA). Norm 9 and 10 are histopathologically verified normal adrenals collected with informed consent at Karolinska University Hospital.

Total lymphocyte DNA from a healthy subject (Norm 11) was used as a control in methylation analyses after hypermethylation *in vitro* by *Sss*I enzyme (New England Biolabs, Ipswich, MA, USA) and subsequent bisulfite treatment. Untreated total lymphocyte DNA constituted the negative control.

Extraction of DNA, RNA, and protein

Tissue samples had been collected according to a standardized procedure, snap frozen in liquid nitrogen, and stored at −70 °C. DNA was extracted by a standard procedure involving phenol–chloroform purification and quantified by regular spectrophotometry (Shimadzu UV-1601) and using a NanoDrop Spectrophotometer (ND-1000). Total RNA was extracted with the Qiagen RNeasy Mini Kit (Cat. No. 74104). RNA integrity was confirmed by means of the Agilent 2100 Bioanalyzer unit and the Agilent RNA 6000 Nano Kit; all samples included in the study displayed electropherograms with distinct *18S* and *28S* peaks. RNA concentration was measured using NanoDrop. Proteins were isolated from frozen tumor tissue by mincing and incubating in sequestration buffer for 1 h on ice. The stock buffer contained 20 mM HEPES, 25% glycerol v/v, 0.42 M NaCl, 1.5 mM $MgCl_2$, 0.4 mM EDTA, and pH was adjusted to 7.9. An aliquot of 1 ml of this buffer was supplemented with 2 µl NP-40 v/v, 0.5 mM dithiothreitol, and 5.35 mg protease inhibitors (Roche). Subsequently, proteins were separated from cell debris by centrifugation at 4 °C, 17 000 ***g*** for 20 min in an Eppendorf 5417R centrifuge. Concentrations were measured using the Bradford method by means of BSA standards. DNA, RNA, and protein extracts were used for studies of methylation, expression, and sequence utilizing oligonucleotides described in Supplementary Table 2 and Fig. 1, which can be viewed online at http://erc.endocrinology-journals.org/supplemental/.

Analyses of promoter methylation

From each sample, 2 µg genomic DNA were bisulfite treated with EZ DNA Methylation Kit (Zymo Research, Orange, CA, USA) and used for MSP and Pyrosequencing.

All MSP reactions were carried out in a GeneAmp PCR 9700 System (Applied Biosystems, Foster City, CA, USA). Methylated $p16^{INK4A}$ promoter was amplified from bisulfite-treated DNA (0.6 µl) with methylation-specific primers (1.8 ng/µl each; Herman *et al*. 1996; Supplementary Table 2) in 25 µl reactions containing 8% dimethyl sulfoxide (DMSO), 0.1 mM of each dNTP, 1.5 mM $MgCl_2$, PCR Gold Buffer (Applied Biosystems), and 2.5 units Taq Gold (Applied Biosystems). The PCR conditions were: 94 °C for 10 min; cycling 35 times at 95 °C for 30 s, 60 °C for 30 s, and 72 °C for 30 s, and 72 °C for 4 min. Similar conditions were applied for the unmethylated-specific reaction, with exception for primer concentration (4.2 ng/µl each), amount of DNA (2.1 µl), DMSO (10%), and annealing temperature (62 °C).

$p14^{ARF}$ promoter sequences were amplified from ∼200 ng bisulfite-treated DNA in 25 µl reactions consisting of 2 µl DMSO, 2.4 ng/µl of each primer (Esteller *et al*. 2000; Supplementary Table 2), 0.1 mM dNTPs, 2.0 mM $MgCl_2$, 2.5 units Taq Gold, and Taq Gold buffer. PCR conditions were 95 °C for 10 min then cycled 35 times at 94 °C for 30 s, 60 °C for 30 s, and 72 °C for 30 s, followed by an extension at 72 °C for 10 min. PCR conditions for the unmethylated primers were similar, except for a 62 °C annealing temperature.

Pyrosequencing assays developed at Biotage AB, Uppsala, Sweden, were used for $p16^{INK4A}$ (REF: 40-0056) and $p14^{ARF}$, applying primers and conditions available at the PyroMark Assay Database (Biotage). Pyrosequencing was performed in a Biotage PSQ 96MA pyrosequencer at Biotage, Uppsala, after verification of amplification products by 3% agarose gel electrophoresis.

cDNA synthesis and quantitative real-time PCR (qRT-PCR)

The methodology for cDNA synthesis, selection of reference housekeeping genes, and qRT-PCR analyses were according to previous publications (Geli *et al*. 2005, 2007). In short, 50 ng cDNA was used in qRT-PCRs performed in an ABI PRISM 7700 Sequence Detection System (SDS, Applied Biosystems). The primer/probe set for $p16^{INK4A}$ span the exon 1α/exon 2 junction (Mark *et al*. 2006), while the set for $p14^{ARF}$ target part of exon 1β (Supplementary Table 2,

Fig. 1). The PCR conditions were as follows: one step cycle with 50 °C for 2 min and 95 °C for 10 min, followed by 40 step cycles of 95 °C for 15 s and 60 °C for 1 min. The housekeeping genes β-2-microglobulin (B2M) and β-actin (ACTB) were amplified using assays on demand Hs00187842_m1 and Hs99999903_m1 respectively (Applied Biosystems). Serial dilutions of cDNA from NAP were amplified in parallel to establish a standard curve for relative quantification. All qRT-PCR experiments were performed in duplicate, including no template controls. The average of the duplicates was used in subsequent calculations.

The raw data were analyzed with the SDS software version 1.9.1. (Applied Biosystems). Following quantification in relation to the generated standard curves, the values were normalized to the geometrical meanof the two housekeeping genes (ACTB and B2M) and subsequently to NAP that was assigned the value of 1.

Western blot analyses

Western blotting was performed in a Bio-Rad PROTEAN II ix Cell system using 10% Tricine gels. Seventy micrograms proteins were loaded to each well. Run time was 2 h at 30 V, followed by 1 h at 100 V, and 3 h at 170 V. The proteins were then blotted overnight at 12 V to Amersham Hybond-P PVDF membranes (Amersham). The membranes were incubated overnight at 4 °C with purified mouse–anti-human p16 primary antibodies (BD Biosciences, Franklin Lakes, NJ, USA Pharmingen Cat. No: 554070) diluted in TBST/dry milk solution to a concentration of 1:100. Membranes were then incubated in room temperature for 60 min together with goat–anti-mouse HRP-conjugated antibody 1:10 000 in TBST/dry milk. The signal was developed with the Amersham Biosciences ECL Western Blotting Detection reagent mixed 2:1 with the ECL Advance Western Blotting Detection reagent, and detected with the Fujifilm Intelligent Dark Box II/LAS 1000 CCD system. To quantify p16, membranes were incubated for 1 h with mouse–anti-human ACTB primary antibodies at a concentration of 1:50 000. Visualization and detection were in the same manner as described above. p16 band intensities were adjusted to those of ACTB for the purpose of normalization using the Image Gauge V3.45 software.

$p16^{INK4A}$ sequencing

All three exons of $p16^{INK4A}$ were sequenced in both directions using primers derived from bordering introns (Supplementary Table 2, Fig. 1). The initial PCR amplification was made in a 25 µl master mix including 1 unit of FinnZymes DyNAzyme EXT DNA polymerase (FinnZymes, Espoo, Finland), 400 nM of each primer, 2.5 µl 10× Buffer (with $MgCl_2$), 160 nM of each dNTP, and 25 ng DNA. The PCR conditions were 95 °C for 10 min, then cycled 35 times at 95 °C for 30 s, an exon-specific annealing temperature for 60 s, and 72 °C for 30 s, followed by a 6-min extension at 72 °C. Annealing temperatures were 60 °C for exon 1, 58 °C for exon 2, and 61 °C for exon 3. After verification by 3% agarose gel electrophoresis and purification using ExoSAP-IT (USB, Cleveland, OH, USA), 1 µl product was added to a master mix containing 1 µl Big Dye Terminator v3.1 (Applied Biosystems), 1.5 µl Sequencing Buffer, and 1 µM primer at a total volume of 10 µl. The thermocycler program was 96 °C for 1 min followed by 25 cycles of 96 °C for 10 s, 50 °C for 4 s, and 60 °C for 4 min. The reactions were run in an Applied Biosystems 3730 DNA Analyzer and coding plus flanking sequences were analyzed with the ABI Prism SeqScape Software v2.5 (Applied Biosystems). For detection of sequence variants, the coding region and neighboring sequences were assessed using the SeqScape software and compared with publicly available 16^{INK4A} sequence (ID OTTHUMT00000051915; Ensembl). Putative sequence variants were confirmed by repeated sequencing.

SDHB sequencing

All exons of the SDHB gene were sequenced using previously published primers (Benn *et al*. 2003, Castellano *et al*. 2006; Supplementary Table 2). Initial PCR was performed using a 25 µl master mix containing 12.5 ng DNA, one unit of AmpliTac Gold, 2.5 µl PCR-buffer II, 200 µM $MgCl_2$ (reagents from Applied Biosystems), 200 nM of each primer, and 80 nM of each dNTP. The PCR conditions were the same for all exons; 9 min and 30 s at 95 °C, eight cycles at 95 °C for 30 s; 62 °C with −1 °C per cycle for 45 s, and 72 °C for 45 s followed by 30 cycles of 95 °C for 30 s, 55 °C for 45 s, and 72 °C for 42 s with a 7-min extension at 72 °C. The PCR was performed on an MJ Research PTC-225 thermocycler (MJ Research, Waltham, MA, USA). Unambiguous amplification was verified on 3% agarose gels, which was followed by product cleanup using ExoSAP-IT (USB). Sequences were run either at the core facility at KiSeq AB (Karolinska Institute, Stockholm, Sweden) or in-house using a capillary-based system (Applied Biosystems 3730 DNA Analyzer). The sequence data was analyzed using the CodonCode Aligner V2.0.2. software (CodonCode Corporation,

Dedham, MA, USA). Mutations were verified by sequencing in the opposite direction.

Statistical analysis

All analyses were performed in STATISTICA (version 7, Statsoft Inc.) and P values <0.05 were considered significant. Mann–Whitney test was used to assess differences in target gene expression relating to gender, pheochromocytomas versus paragangliomas, tumors with no evidence of malignancy versus tumors classified as malignant, syndromic or non-syndromic presentation, SDHB mutation status, and target gene promoter methylation. Correlation between target gene expression/methylation density and age at presentation or tumor size was examined using Spearman Rank Order Correlations. Fisher's exact test was used for correlation analyses between $p16^{INK4A}$ MSP data and categorical clinical parameters. $p16^{INK4A}$ methylation determined by MSP and Pyrosequencing were compared by Mann–Whitney.

Results

In this study, $p16^{INK4A}$ and $p14^{ARF}$ promoter methylation were investigated together with expression levels and sequence analyses in 57 pheochromocytomas and paragangliomas from 55 patients. The findings were subsequently evaluated in relation to clinical characteristics and SDHB mutation.

Promoter methylation analyses of $p16^{INK4A}$ and $p14^{ARF}$

$p16^{INK4A}$ and $p14^{ARF}$ promoter methylation was qualitatively assessed by MSP and quantified by Pyrosequencing (Fig. 2). In control experiments using MSP, DNA *in vitro* hypermethylated with *Sss*I yielded the expected product using the methylation-specific primers, while non-*Sss*1-treated DNA only gave a product with primers for the non-methylated state. In addition, normal DNA without bisulfite treatment was completely negative. Normal adrenal DNA was found to have very low levels of methylation for both $p16^{INK4A}$ and $p14^{ARF}$.

Seven tumor samples from five patients showed extensive $p16^{INK4A}$ methylation for the four CpG sites assessed, without preferential involvement of any individual site (Table 2). The individual values ranged from 11 to 70%, and the means of the four CpG sites were between 22 and 67%. This finding was in complete agreement with the MSP analyses that detected $p16^{INK4A}$ methylation in the same seven tumors only ($P=0.000001$; Fig. 2). The two pairs of

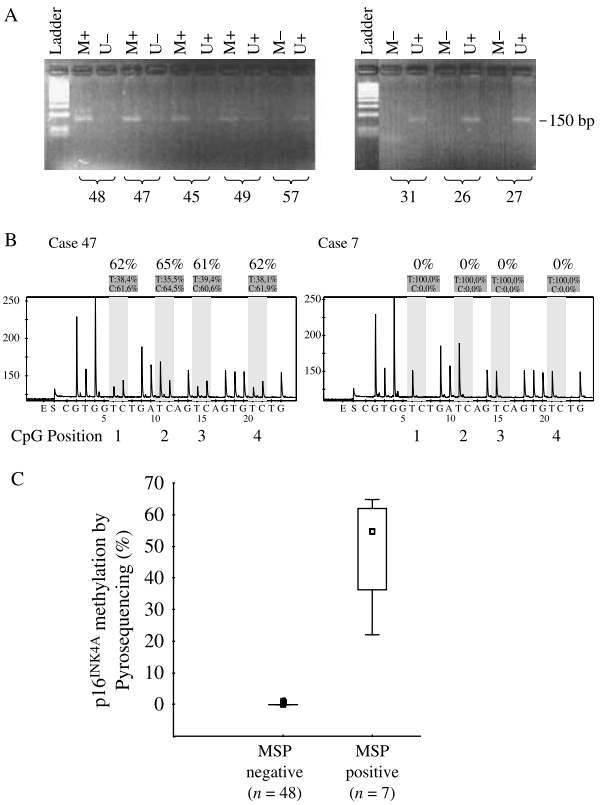

Figure 2 Detection of $p16^{INK4A}$ promoter hypermethylation in pheochromocytoma and paraganglioma. (A) Methylation-specific PCR (MSP) showing methylated and unmethylated PCR products for eight tumors. (B) Pyrograms illustrating the four CpG-s in the p16(INK4A) promoter. Sample 47 shows ~60% methylation in the assessed CpG sites, while sample 7 is showing 0% methylation in the same CpGs. (C) Box plot illustrating the high concordance in the detection of $p16^{INK4A}$ methylation between the two methods.

matched primary tumor and metastasis both showed high levels of $p16^{INK4A}$ methylation. In the remaining tumors, $p16^{INK4A}$ methylation was not detected by either of the methods.

In contrast, only very low levels of $p14^{ARF}$ promoter methylation were revealed in the tumors. The initial MSP analyses indicated that $p14^{ARF}$ promoter methylation was present in 42 out of the 57 tumors (73%; Table 2). However, at subsequent Pyrosequencing, $p14^{ARF}$ methylation levels were found to be very low. The mean methylation level of the 13 CpGs analyzed ranged from 0.0 to 4.8% for the individual samples. One sample (no. 6) was completely devoid of methylation in each of the assessed CpGs, and values above 10% were only recorded in two instances at individual CpG sites. Thus, low levels of $p14^{ARF}$ methylation were found in the majority of tumors and were within the same range as those measured in normal controls.

Table 2 Results from analyses of $p16^{INK4A}$ and $p14^{ARF}$ and their expression in tumor samples

		Analyses of $p16^{INK4A}$					Analyses of $p14^{ARF}$		
				Expression				Pyro CpG 1–13	
Sample no. – type	Criteria for malignancy	MSP	Prosequencing CpG 1–4 (%)	mRNA	Western	DNA sequence	MSP	Mean (Range %)	mRNA
Tumors with no evidence of malignancy									
1 – phe	–	No	0/0/0/0	1.88	+	wt	Yes	1.0 (0.0–2.1)	2.32
2 – phe	–	No	0/0/0/0	0.43	+	wt	Yes	0.9 (0.0–2.4)	0.97
3 – phe	–	No	0/0/0/0	0.09	(+/−)	wt	Yes	1.5 (0.0–8.8)	0.44
4 – phe	–	No	0/0/0/0	0.38	(+/−)	wt	No	2.5 (0.0–7.0)	0.63
5 – phe	–	No	0/0/0/0	0.15	(+/−)	wt	Yes	2.0 (0.0–2.6)	0.76
6 – phe	–	No	0/0/0/0	0.38	+	wt	No	0.0 (0.0–0.0)	0.80
7 – phe	–	No	0/0/0/0	0.43	+	wt	Yes	4.5 (0.0–19.7)	0.50
8 – parag	–	Yes	47/27/13/59	1.20	+	wt	Yes	1.8 (0.0–2.8)	0.76
9 – phe	–	No	n/a	0.91	n/a	wt	Yes	1.7 (0.0–2.7)	0.76
10 – phe	–	No	0/0/0/0	0.79	+	wt	Yes	1.5 (0.0–2.4)	0.72
11 – phe	–	No	0/0/0/0	0.72	+	wt	Yes	1.7 (0.0–2.7)	0.38
12 – phe	–	No	0/0/0/0	0.46	+	wt	No	1.4 (0.0–2.8)	1.02
13 – phe	–	No	0/0/0/0	0.49	(+/−)	wt	No	1.3 (0.0–5.0)	0.57
14 – phe	–	No	0/0/0/0	0.89	(+/−)	A148T	Yes	1.1 (0.0–2.3)	1.00
15 – phe	–	No	0/0/0/0	0.32	(+/−)	wt	Yes	1.4 (0.0–2.2)	0.90
16 – phe	–	No	0/0/0/0	1.96	+	A148T	No	1.4 (0.0–2.2)	2.37
17 – phe	–	No	0/0/0/0	2.75	+	wt	Yes	0.5 (0.0–1.7)	2.25
18 – phe	–	No	0/0/0/0	0.83	++	A57V	No	0.6 (0.0–1.8)	0.95
19 – phe	–	No	0/0/0/0	0.52	+	wt	No	2.0 (0.0–3.2)	0.88
20 – phe	–	No	0/0/0/0	0.67	++	wt	No	0.6 (0.0–2.5)	0.90
21 – parag	–	No	0/0/0/0	0.23	(+/−)	wt	No	1.6 (0.0–4.4)	0.78
22 – phe	–	No	0/0/0/0	0.79	+	wt	Yes	2.3 (0.0–8.3)	0.79
23 – phe	–	No	0/0/0/0	2.28	++	wt	No	1.9 (0.0–3.6)	4.53
24 – parag	–	No	0/0/0/0	3.48	+	wt	Yes	0.4 (0.0–1.5)	n/a
25 – phe	–	No	5/0/0/0	1.01	++	wt	Yes	1.6 (0.0–3.8)	1.15
26 – phe	–	No	0/0/0/0	0.62	+	wt	Yes	1.3 (0.0–2.3)	1.56
27 – phe	–	No	0/0/0/0	2.52	+	wt	Yes	1.4 (0.0–2.6)	1.95
28 – parag	–	No	0/0/0/0	2.66	+	wt	Yes	1.2 (0.0–2.5)	2.62
29 – phe	–	No	4/0/0/0	0.34	(+/−)	wt	Yes	3.9 (0.0−9.4)	0.65
30 – parag	–	No	0/0/0/0	0.18	(+/−)	wt	No	1.3 (0.0–2.8)	0.70
31 – phe	–	No	0/0/0/0	0.16	+	wt	Yes	2.5 (0.0–5.4)	0.31
32 – phe	–	No	0/0/0/0	0.81	+	wt	Yes	2.0 (0.0–3.0)	0.59
33 – phe	–	No	0/0/0/0	1.30	+	wt	Yes	1.3 (0.0–2.0)	5.41
34 – phe	–	No	0/0/0/0	0.33	+	wt	No	1.8 (0.0–3.3)	0.28
35 – phe	–	No	0/0/0/0	0.77	+	wt	Yes	2.5 (1.4–3.4)	2.72
36 – parag	–	No	0/0/0/0	0.20	+	wt	Yes	1.4 (0.0–2.6)	0.20
37 – phe	–	No	0/0/0/0	2.14	++	wt	Yes	2.2 (0.0–7.0)	1.98
38 – phe	–	No	0/0/0/0	0.43	(+/−)	A148T	Yes	1.6 (0.0–2.8)	0.28
39 – phe	–	No	0/0/0/0	0.62	+	wt	Yes	0.7 (0.0–2.6)	0.73
40 – phe	–	No	0/0/0/0	1.74	+	wt	Yes	0.9 (0.0–2.5)	1.61
41 – phe	–	No	0/0/0/0	0.05	(+/−)	wt	Yes	4.8 (0.0–30.0)	0.08
42 – phe	–	No	0/0/0/0	0.94	++	wt	Yes	2.3 (0.0–5.0)	1.19
43 – phe	–	No	0/0/0/0	n/a	+	wt	Yes	1.5 (0.0–2.5)	2.42
44 – phe	–	No	0/0/0/0	n/a	n/a	wt	Yes	n/a	1.08
Tumors classified as malignant									
45 – parag	Met	Yes	60/56/33/58	0.80	+	wt	Yes	3.1 (0.0–4.9)	6.63
46 – parag	Met	No	0/0/0/0	0.34	+	wt	Yes	0.4 (0.0–1.7)	1.96
47 – parag	Met	Yes	62/65/61/62	0.54	+	wt	Yes	1.3 (0.0–2.6)	4.41
48 – met	–	Yes	56/54/54/56	n/a	+	wt	Yes	0.4 (0.0–1.8)	9.67
49 – parag	Met	Yes	70/65/55/70	0.18	(+/−)	wt	Yes	0.9 (0.0–2.0)	5.26
50 – parag	Loc. inv.	Yes	27/11/18/32	0.11	+	wt	No	1.8 (0.0–2.5)	n/a
51 – met	–	Yes	57/60/57/58	0.16	(+/−)	wt	Yes	0.4 (0.0–1.3)	5.53

Table 2 *continued*

		Analyses of $p16^{INK4A}$					Analyses of $p14^{ARF}$		
				Expression				Pyro CpG 1–13	
Sample no. – type	Criteria for malignancy	MSP	Prosequencing CpG 1–4 (%)	mRNA	Western	DNA sequence	MSP	Mean (Range %)	mRNA
52 – phe	Loc. inv.	No	0/0/0/0	0.53	(+/−)	wt	No	1.6 (0.0–2.8)	0.49
53 – phe	Loc. inv.	No	0/0/0/0	0.20	(+/−)	wt	Yes	1.8 (0.0–3.0)	0.23
54 – phe	Met	No	0/0/0/0	0.29	+	wt	No	2.7 (0.0–7.5)	0.83
55 – phe	Met	No	0/0/0/0	0.08	++	wt	Yes	1.2 (0.0–2.6)	0.21
56 – phe	Loc. inv.	No	0/0/0/0	0.83	+	wt	Yes	1.7 (0.0–4.5)	1.41
57 – phe	Loc. inv.	No	0/0/0/0	0.62	(+/−)	wt	Yes	1.7 (0.0–7.0)	0.66

n/a, not analysed/not available; phe, pheochromocytoma; parag, abdominal araganglioma; +/−, reduced or lost; +, normal range; ++, increased expression compared to normal drenals; MSP, methylation-specific PCR. mRNA expression values are in relation to the value 1.0 assigned to NAP. Met, metastasis; Loc. inv., local invasion; −, not applicable.

$p16^{INK4A}$ and $p14^{ARF}$ expression

Gene expression levels were determined in tumors and normal tissues applying qRT-PCR assays for distinct analysis of the CDKN2A transcripts (Fig. 1). Overall, no significant difference in $p16^{INK4A}$ or $p14^{ARF}$ expression was observed between the tumor panel and normal adrenal medullary samples (Norm 5–8; Tables 1 and 2). However, tumors classified as malignant tended to have lower $p16^{INK4A}$ expression than normal adrenal medullary samples ($P=0.0502$).

p16 protein expression

For the sake of arbitration, p16 band intensities were normalized against corresponding ACTB bands. Samples were then compared with Norm 10 (the highest scoring normal adrenal sample), and then scored as having unaltered (+; 50–150% of Norm 10), lost or reduced (+/−; <50% of Norm 10), or increased (++; >150% of Norm 10) p16 expression as exemplified in Fig. 3. Increased (++) p16 expression of an expected ~18 kDa product was confirmed in SAOS-2 cells used as a positive control, while the negative control MCF-7 showed no p16 expression (Fig. 3). Sixteen tumors exhibited lost or reduced p16 protein expression (+/−) when compared with that measured in normal whole adrenals (Table 2; Fig. 3). In 33 tumors, the level was scored as unaltered (+), while in 7 tumors the expression was increased (++).

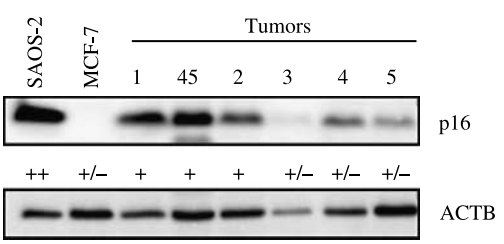

Figure 3 Western blot analyses showing p16 protein levels in control cells and tumor samples. The expression was scored as increased (++), unaltered (+), or lost/decreased (+/−) as indicated. Quantification was performed against ACTB shown below to ensure an unbiased assessment of protein level.

$p16^{INK4A}$ sequence variants and mutations

Analysis of the coding region and flanking sequences of $p16^{INK4A}$ revealed sequence alterations in four of the 57 tumors analyzed (Fig. 4; Table 2). In tumor 18, a previously reported (https://biodesktop.uvm.edu/perl/p16) missense mutation A57V was observed resulting from a substitution GCC>GTC in exon 2 (silent in $p14^{ARF}$). Furthermore, a known SNP, A148T (rs3731249), was found in tumors 14, 16, and 38 (5%; this mutation falls outside the coding sequence of $p14^{ARF}$). No sequence variations were detected in exons 1 and 3, nor their flanking splice junctions.

SDHB mutations

The SDHB gene was screened for mutations in all samples classified as malignant ($n=13$), in paragangliomas with no evidence of malignancy ($n=5$), and in tumors from patients with early age of presentation (≤30 years; $n=3$). In total, 5 out of the 21 tumors analyzed exhibited an SDHB mutation (Supplementary Table 1; Supplementary Fig. 1). In case 8, a single nucleotide deletion of a G at position 190 (c.190delG) in exon 1 was observed and predicted to lead to a frameshift from codon 64. Frameshift mutations with duplication of four nucleotides (c.151_154insGACA) in exon 2 were found in cases 49 and 50, and a splice

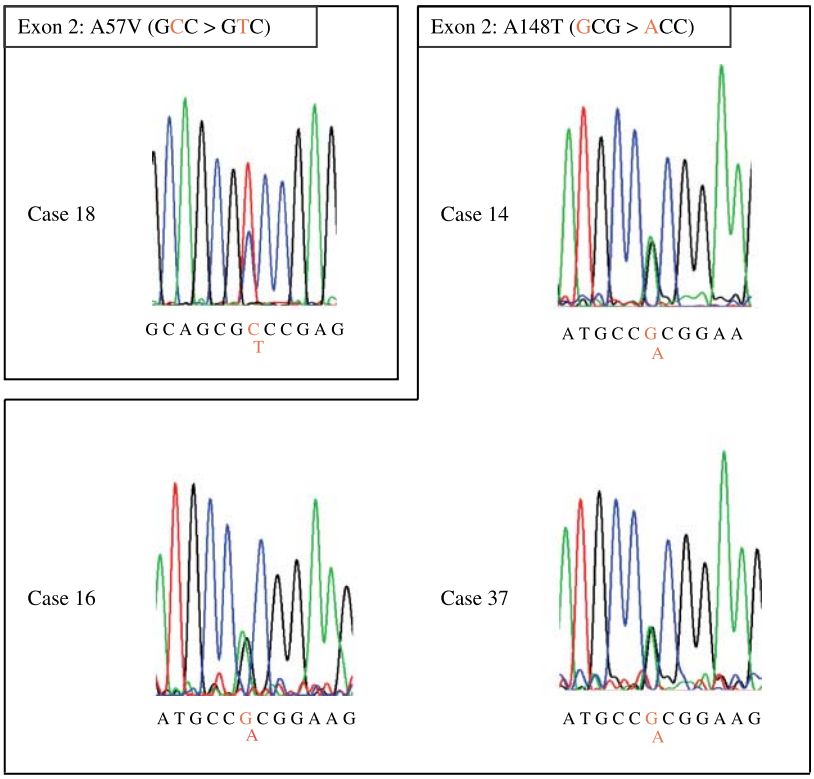

Figure 4 p16^{INK4A} sequence electropherograms showing the sequence alterations detected in four tumors. For tumor 18, the electropherogram represents the reverse sequencing analyses after inversion. Nucleotide substitutions are revealed as double peaks and are indicated with red letters.

site mutation (c.423+1G>A) was detected at the exon 4–intron 4 border in primary tumor 47 and its metastasis 51. A non-functional SNP (c.18A>C) was observed in case 50.

p16^{INK4A} hypermethylation and gene suppression in association with malignancy and SDHB mutation

All findings from studies of methylation, expression, and sequence were evaluated in relation to the clinical characteristics of the 55 primary tumors. From these comparisons, several statistically significant associations were observed. p16^{INK4A} promoter methylation was significantly associated with malignant disease ($P=0.0043$; Fig. 5), as four out of the five cases with p16^{INK4A} methylation represented tumors classified as malignant plus matching metastasis. Furthermore, tumors classified as malignant had significantly lower p16^{INK4A} mRNA expression compared with tumors with no evidence of malignancy ($P<0.05$; Fig. 5). In relation to the classification of tumors as pheochromocytoma or paraganglioma, p16^{INK4A} hypermethylation was found to be over-represented among paragangliomas ($P=0.0001$). Paragangliomas also showed higher levels of p14^{ARF} expression when compared with pheochromocytomas ($P=0.02$). A statistically significant association was shown between p16^{INK4A} methylation and the presence of SDHB gene mutation ($P<0.002$) whereby all cases with SDHB mutation also featured p16^{INK4A} methylation.

Discussion

In this study, we report promoter hypermethylation and reduced gene expression of p16^{INK4A} in association with malignant disease. In addition, a subset of tumors exhibited reduced p16 protein expression, and one case harbored a missense p16^{INK4A} mutation. The CDKN2A gene locus was originally implicated in pheochromocytomas based on findings in mouse Ink4a/Arf Pten+/− knockout models (You *et al.* 2002). The conclusion from these studies was that the combined loss of function for Pten together with p16/p14 promotes the development of pheochromocytomas concerning onset, multiplicity, and aggressiveness. However, the loss of p16/p14 alone was not sufficient for tumor development in this model. In the present study, we observed recurrent alterations of p16^{INK4A} in human

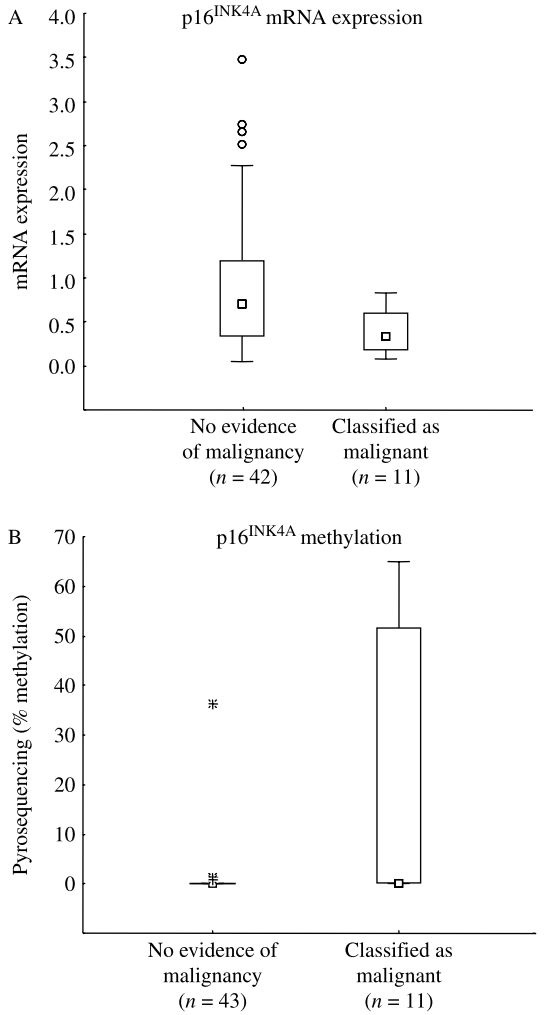

Figure 5 Box plots illustrating associations between malignant disease and (A) suppressed $p16^{INK4A}$ mRNA expression levels (normalized to NAP = 1) and (B) hypermethylation of the $p16^{INK4A}$ promoter in the primary tumors.

pheochromocytomas and paragangliomas, without apparent involvement of $p14^{ARF}$. The findings confirm an involvement of the CDKN2A locus in human forms of these tumors and identify $p16^{INK4A}$ as the relevant target, while at the same time vindicating $p14^{ARF}$. Our findings support that $p16^{INK4A}$ and $p14^{ARF}$ are separately involved in tumor development, as was recently demonstrated for colon cancer where $p16^{INK4A}$ and $p14^{ARF}$ methylation frequencies vary between different forms of the disease (Kaz *et al*. 2007).

A significant association was observed between $p16^{INK4A}$ promoter hypermethylation and malignant disease. In addition, using a quantitative approach, high levels of $p16^{INK4A}$ methylation were demonstrated in malignant tumor samples. This implies that $p16^{INK4A}$ promoter hypermethylation is likely to be of biological relevance, in contrast to $p14^{ARF}$ for which methylation was frequently recorded, albeit only at low levels comparable with corresponding normal tissues.

The findings also illustrate the value of applying a quantitative approach (such as Pyrosequencing) in addition to qualitative methods (such as MSP) for assessment of methylation levels. The methodological differences relate mainly to the high sensitivity of the MSP method by which very low levels of methylation that are of questionable biological significance can be detected. In our own experience, *in vitro* hypermethylated DNA is detectable even after high dilution, in agreement with Herman *et al*. (1996). The quantitative Pyrosequencing technique is likely to evolve into a versatile tool for epigenetic research and diagnostic purposes (Konishi *et al*. 2007).

Notably, $p16^{INK4A}$ promoter hypermethylation was only observed in paragangliomas and not pheochromocytomas. More specifically, four out of the five primary paragangliomas with $p16^{INK4A}$ hypermethylation were classified as malignant, indicating an association between $p16^{INK4A}$ hypermethylation and malignancy. However, given the limited number of samples, this notion should be confirmed in larger independent series. In this study, the AFIP criteria were used for the establishment of malignancy, i.e., the diagnosis of malignancy requires the presence of distant metastases and/or extensive local invasion (Lack 1997). Another widely accepted classification system is that of the WHO, i.e., only the presence of distant metastases is acknowledged as proof of metastasis (Thompson *et al*. 2004). In our study, three out of the four malignant primary paragangliomas with p16 hypermethylation developed metastases (Supplementary Table 1; tumors 45, 47, 49 and metastases 48 and 51). However, initially two of these were characterized only by local invasion (Tumors 45 and 47) and only later developed metastases. Tumors such as these would have been diagnosed as benign at initial evaluation using WHO criteria. In contrast, some cases classified as malignant based on extensive local invasion only (according to AFIP criteria) remain disease free during follow-up. The significance of local invasion remains to be determined in clinical and genetic subgroups of pheochromocytoma and paraganglioma patients. Similar levels of $p16^{INK4A}$ promoter hypermethylation were observed in distant metastases as in their primary counterparts, indicating that this is an early event in tumorigenesis. However, it is possible that $p16^{INK4A}$ methylation is an effect of a somatic mutation in a gene involved in methylation patterning. The lack of demonstrable $p16^{INK4A}$ mutations in hypermethylated

cases indicates that such a putative gene is different from $p16^{INK4A}$. In this context, it is interesting to note that four out of the five primary tumors displaying $p16^{INK4A}$ promoter methylation harbored SDHB mutations ($P<0.002$), and that all tumors with detected SDHB mutation had methylated $p16^{INK4A}$ promoters, including a benign paraganglioma (Case 8). All of the affected samples have at least one disrupting alteration of the SDHB sequence, including deletion, insertions, and a novel splice mutation (c.423+1G>A) in a previously reported site, which was described by the authors as a 'splice defect' (Amar *et al*. 2005). Although based on a limited number of observations, our data suggest a possible association between SDHB mutation and $p16^{INK4A}$ promoter hypermethylation, which remains to be verified in an independent series and mechanistically tested.

Generally, transcriptional suppression of a negative cell-cycle regulator such as $p16^{INK4A}$ is considered as an event favoring neoplastic growth. This is in agreement with our observation of significantly lower $p16^{INK4A}$ mRNA expression in malignant tumors compared with benign ones (Fig. 5; Table 2). In benign tumors, considerable variation in expression level was seen with no apparent further association to clinical features. At the protein level 16, tumors showed lost or reduced p16 expression that in all cases was reflected by decreased mRNA abundance on the transcriptional level. However, in some tumors, p16 protein and mRNA levels did not correlate well with each other. Similar results have been obtained for other tumors concerning expression at the CDKN2A locus, as demonstrated in a recent study by Brownhill *et al* (2007). Poor correlation between mRNA and protein expression is in fact a common phenomenon as has been shown previously in tumors and model system (Gygi *et al*. 1999, Chen *et al*. 2002), and may result from varying transcript stability, post-transcriptional modifications, or reflect intra-tumor variations. Likewise, tumor heterogeneity may explain seemingly unaltered mRNA expression in tumors with a high degree of $p16^{INK4A}$ promoter methylation (samples 8, 45, and 47). Inconsistencies between $p16^{INK4A}$ promoter methylation status and mRNA expression have been reported previously (Hardie *et al*. 2005, Liu *et al*. 2005).

$p16^{INK4A}$ sequence variations were detected in four tumors, which all caused amino acid changes. The missense alteration A57V has been previously reported as a germline mutation as well as in a few cases of hematological and other malignancies (https://biodesk-top.uvm.edu/perl/p16). In our study, this variation was detected in a patient diagnosed with pheochromocytoma at 30 years of age and who had previously been treated for a prolactinoma. The known SNP, A148T found in three tumors (5%) is reported in 6% of the global and 3% of the European population (http://www.ncbi.nlm.nih.gov/SNP/snp_ref.cgi?rs=3731249). It has also been reported as a predisposing alteration in connection to malignant melanoma and breast and lung cancer (Debniak *et al*. 2005, 2006, Puig *et al*. 2005). None of the detected sequence alterations occurred in conjunction with malignant disease. Taken together with previous reports showing lack of somatic loss of the CDKN2A locus (Aguiar *et al*. 1996), we can conclude that genomic alterations in $p16^{INK4A}$ do not commonly promote malignancy in human pheochromocytomas and paragangliomas; however, their presence may enhance the rate of neoplastic formation.

In conclusion, $p16^{INK4A}$ promoter methylation was almost exclusively found in malignant cases and could therefore reflect an important event in the development of malignancy in these tumor types. This stands in good agreement with the findings of You *et al*. that pheochromocytoma-prone mice with homozygous Ink4a/Arf inactivation often develop metastases. The recognition of malignant disease in pheochromocytoma and paraganglioma is a long-lasting tumblingstone. The first problem relates to the diagnostic criteria, i.e., whether metastatic disease is a requirement or whether the malignant entity should also include tumors that feature only extensive local invasion. Secondly, since malignancy often cannot readily be detected at diagnosis, all patients are virtually at risk of developing malignant disease with metastases during follow-up. Hence, the development of novel biomarkers for malignant behavior is warranted. If our findings can be verified in an independent material, assessment of $p16^{INK4A}$ promoter hypermethylation could be used as an additional tool to assess increased risk for malignant behavior. In a longer perspective, these findings could have implications for novel adjuvant therapeutic strategies based on demethylating agents in the treatment of malignant disease. Further elucidation of the $p16^{INK4A}$ and interacting molecules in pheochromocytoma and paraganglioma may aid the identification of novel molecular targets to combat cancer.

Acknowledgements

The authors would like to thank Professor Bertil Hamberger and Dr Elisabeth Edström-Elder for expert clinical evaluation of the cases, Lisa Åhnfalk for excellent help in tumor collection, Dr Tzvetomira Philipova and Dr Tatjana Yakolevafor expert technical advice, and Annika Eriksson at KiSeq for her substantial help in sequencing SDHB. Pyrosequencing

was carried out in collaboration with Biotage AB as detailed in Materials and methods. No financial or other kind of support was received from Biotage AB that would compromise the impartiality of this study. The authors declare that there is no conflict of interest that would prejudice the objectivity of this scientific work. This study was financially supported by Swedish Cancer Society, Göran Gustafsson Foundation for Research in Natural Sciences and Medicine, Gustav V Jubilee Foundation, Stockholm Cancer Society, Karolinska Institutet, and Stockholm County Council.

References

Aguiar RC, Dahia PL, Sill H, Toledo SP, Goldman JM & Cross NC 1996 Deletion analysis of the p16 tumour suppressor gene in phaeochromocytomas. *Clinical Endocrinology* **45** 93–96.

Amar L, Bertherat J, Baudin E, Ajzenberg C, Bressac-de Paillerets B, Chabre O, Chamontin B, Delemer B, Giraud S & Murat A 2005 Genetic testing in pheochromocytoma or functional paraganglioma. *Journal of Clinical Oncology* **23** 8812–8818.

Antequera F, Boyes J & Bird A 1990 High levels of de novo methylation and altered chromatin structure at CpG islands in cell lines. *Cell* **62** 503–514.

Baylin SB, Herman JG, Graff JR, Vertino PM & Issa J-P 1998 Alterations in DNA methylation: a fundamental aspect of neoplasia. *Advances in Cancer Research* **72** 141–196.

Benn DE, Croxson MS, Tucker K, Bambach CP, Richardson AL, Delbridge L, Pullan PT, Hammond J, Marsh DJ & Robinson BG 2003 Novel succinate dehydrogenase subunit B (SDHB) mutations in familial phaeochromocytomas and paragangliomas, but an absence of somatic SDHB mutations in sporadic phaeochromocytomas. *Oncogene* **22** 1358–1364.

Brownhill SC, Taylor C & Burchill SA 2007 Chromosome 9p21 gene copy number and prognostic significance of p16 in ESFT. *British Journal of Cancer* **96** 1914–1923.

Bryant J, Farmer J, Kessler LJ, Townsend RR & Nathanson KL 2003 Pheochromocytoma: the expanding genetic differential diagnosis. *Journal of National Cancer Institute* **95** 1196–1204.

Castellano M, Mori L, Giacchè M, Agliozzo E, Tosini R, Panarotto A, Cappelli C, Mulatero P, Cumetti D, Veglio F *et al.* 2006 Genetic mutation screening in an italian cohort of nonsyndromic pheochromocytoma/paraganglioma patients. *Annals of the New York Academy of Sciences* **1073** 156–165.

Chen G, Gharib TG, Huang CC, Taylor JM, Misek DE, Kardia SL, Giordano TJ, Iannettoni MD, Orringer MB, Hanash SM *et al.* 2002 Discordant protein and mRNA expression in lung adenocarcinomas. *Molecular and Cellular Proteomics* **1** 304–313.

Dammann R, Schagdarsurengin U, Seidel C, Trümpler C, Hoang-Vu C, Gimm O, Dralle H, Pfeifer GP & Brauckhoff M 2005 Frequent promoter methylation of tumor-related genes in sporadic and men2-associated pheochromocytomas. *Experimental and Clinical Endocrinology and Diabetes* **113** 1–7.

Debniak T, Gorski B, Huzarski T, Byrski T, Cybulski C, Mackiewicz A, Gozdecka-Grodecka S, Gronwald J, Kowalska E, Haus O *et al.* 2005 A common variant of CDKN2A (p16) predisposes to breast cancer. *Journal of Medical Genetics* **42** 763–765.

Debniak T, Scott RJ, Huzarski T, Byrski T, Rozmiarek A, Debniak B, Gorski B, Cybulski C, Medrek K, Mierzejewski M *et al.* 2006 CDKN2A common variant and multi-organ cancer risk – a population-based study. *International Journal of Cancer* **118** 3180–3182.

Edström E, Mahlamaki E, Nord B, Kjellman M, Karhu R, Höög A, Goncharov N, Teh BT, Bäckdahl M & Larsson C 2000 Comparative genomic hybridization reveals frequent losses of chromosomes 1p and 3q in pheochromocytomas and abdominal paragangliomas, suggesting a common genetic etiology. *American Journal of Pathology* **156** 651–659.

Edström-Elder E, Hjelm-Skog AL, Höög A & Hamberger B 2003 The management of benign and malignant pheochromocytoma and abdominal paraganglioma. *European Journal of Surgery and Oncology* **29** 278–283.

Elder EE, Elder G & Larsson C 2005 Pheochromocytoma and functional paraganglioma syndrome: no longer the 10% tumor. *Journal of Surgical Oncology* **89** 193–201.

Esteller M 2003 Cancer epigenetics: DNA methylation and chromatin alterations in human cancer. *Advances in Experimental Medicine and Biology* **532** 39–49.

Esteller M 2005 Aberrant DNA methylation as a cancer-inducing mechanism. *Annual Review of Pharmacology and Toxicology* **45** 629–656.

Esteller M, Tortola S, Toyota M, Capella G, Peinado MA, Baylin SB & Herman JG 2000 Hypermethylation-associated inactivation of p14(ARF) is independent of p16(INK4a) methylation and p53 mutational status. *Cancer Research* **60** 129–133.

Esteller M, Corn PG, Baylin SB & Herman JG 2001 A gene hypermethylation profile of human cancer. *Cancer Research* **61** 3225–3229.

Feinberg AP & Tycko B 2004 The history of cancer epigenetics. *Nature Reviews. Cancer* **4** 143–153.

Geli J, Nord B, Frisk T, Edström Elder E, Ekström TJ, Carling T, Bäckdahl M & Larsson C 2005 Deletions and altered expression of the RIZ1 tumour suppressor gene in 1p36 in pheochromocytomas and abdominal paragangliomas. *International Journal of Oncology* **26** 1385–1391.

Geli J, Kiss N, Lanner F, Foukakis T, Natalishvili N, Larsson O, Kogner P, Höög A, Clark GJ, Ekström TJ *et al.* 2007 The Ras effectors NORE1A and RASSF1A are frequently inactivated in pheochromocytoma and abdominal paraganglioma. *Endocrine-Related Cancer* **14** 125–134.

Gygi SP, Rochon Y, Franza BR & Aebersold R 1999 Correlation between protein and mRNA abundance in yeast. *Molecular and Cellular Biology* **19** 1720–1730.

Hardie LJ, Darnton SJ, Wallis YL, Chauhan A, Hainaut P, Wild CP & Casson AG 2005 p16 expression in Barrett's

esophagus and esophageal adenocarcinoma: association with genetic and epigenetic alterations. *Cancer Letters* **217** 221–230.

Herman JG, Graff JR, Myohanen S, Nelkin BD & Baylin SB 1996 Methylation-specific PCR: a novel PCR assay for methylation status of CpG islands. *PNAS* **93** 9821–9826.

Holliday R & Grigg GW 1993 DNA methylation and mutation. *Mutation Research* **285** 61–67.

Kaz A, Kim YH, Dzieciatkowski S, Lynch H, Watson P, Kay Washington M, Lin L & Grady WM 2007 Evidence for the role of aberrant DNA methylation in the pathogenesis of Lynch syndrome adenomas. *International Journal of Cancer* **120** 1922–1929.

Kimura N, Chetty R, Capella C, Young WF Jr, Koch CA, Lam KY, DeLellis RA, Kawashima A, Komminoth P & Tischler AS 2004 Extra-adrenal paraganglioma: carotid body, jugulotympanic, vagal, laryngeal, aortico-pulmonary. In *World Health Organization Classification of Tumors. Pathology and Genetics of Tumors of Endocrine Organs*, pp 159–161. Eds RA DeLellis, RV Lloyd, PU Heitz & C Eng. Lyon: IARC Press.

Konishi K, Shen L, Wang S, Meltzer SJ, Harpaz N & Issa JP 2007 Rare CpG island methylator phenotype in ulcerative colitis-associated neoplasias. *Gastroenterology* **132** 1254–1260.

Lack EE 1997 *Tumors of the Adrenal Gland and Extra-Adrenal Paraganglia*. Washington, DC: Armed Forces Institute of Pathology.

Liu Z, Wang LE, Wang L, Lu KH, Mills GB, Bondy ML & Wei Q 2005 Methylation and messenger RNA expression of p15INK4b but not p16INK4a are independent risk factors for ovarian cancer. *Clinical Cancer Research* **11** 4968–4976.

Mao L, Merlo A, Bedi G, Shapiro GI, Edwards CD, Rollins BJ & Sidransky D 1995 A novel p16INK4A transcript. *Cancer Research* **55** 2995–2997.

Mark EB, Jonsson M, Asp J, Wennberg AM, Mölne L & Lindahl A 2006 Expression of genes involved in the regulation of p16 in psoriatic involved skin. *Archives of Dermatological Research* **297** 459–467.

McCabe DC & Caudill MA 2005 DNA methylation, genomic silencing, and links to nutrition and cancer. *Nutrition Reviews* **63** 183–195.

Nakamura E & Kaelin WG 2006 Recent insights into the molecular pathogenesis of pheochromocytoma and paraganglioma. *Endocrine Pathology* **17** 97–106.

Neumann HP, Bausch B, McWhinney SR, Bender BU, Gimm O, Franke G, Schipper J, Klisch J, Altehoefer C, Zerres K *et al.* 2002 Germ-line mutations in nonsyndromic pheochromocytoma. *New England Journal of Medicine* **346** 1459–1466.

Neumann HP, Pawlu C, Peczkowska M, Bausch B, McWhinney SR, Muresan M, Buchta M, Franke G, Klisch J, Bley TA *et al.* 2004 Distinct clinical features of paraganglioma syndromes associated with SDHB and SDHD gene mutations. *Journal of the American Medical Association* **292** 943–951.

Puig S, Malvehy J, Badenas C, Ruiz A, Jimenez D, Cuellar F, Azon A, Gonzalez U, Castel T & Campoy A 2005 Role of the CDKN2A locus in patients with multiple primary melanomas. *Journal of Clinical Oncology* **23** 3043–3051.

Quelle DE, Zindy F, Ashmun RA & Sherr CJ 1995 Alternative reading frames of the INK4a tumor suppressor gene encode two unrelated proteins capable of inducing cell cycle arrest. *Cell* **83** 993–1000.

Rocco JW & Sidransky D 2001 p16(MTS-1/CDKN2/INK4a) in cancer progression. *Experimental Cell Research* **264** 42–55.

Serrano M, Hannon GJ & Beach D 1993 A new regulatory motif in cell-cycle control causing specific inhibition of cyclin D/CDK4. *Nature* **366** 704–707.

Sharpless NE 2005 INK4a/ARF: a multifunctional tumor suppressor locus. *Mutation Research* **576** 22–38.

Sharpless NE & DePinho RA 1999 The INK4A/ARF locus and its two gene products. *Current Opinion in Genetics & Development* **9** 22–30.

De Smet C, Lurquin C, Lethé B, Martelange V & Boon T 1999 DNA methylation is the primary silencing mechanism for a set of germ line- and tumor-specific genes with a CpG-rich promoter. *Molecular and Cellular Biology* **19** 7327–7335.

Thompson LDR, Young WF Jr, Kawashima A, Komminoth P & Tischler AS 2004 Malignant adrenal pheochromocytomas. In *World Health Organization Classification of Tumors. Pathology and Genetics of Tumors of Endocrine Organs*, pp 147–150. Eds RA DeLellis, RV Lloyd, PU Heitz & C Eng. Lyon: IARC Press.

Tischler AS, Komminoth P, Kimura N & Young WF Jr 2004 Extra-adrenal paraganglioma: gangliocytic, cauda equina, orbital, nasopharyngeal. In *World Health Organization Classification of Tumors. Pathology and Genetics of Tumors of Endocrine Organs*, pp 162–163. Eds RA DeLellis, RV Lloyd, PU Heitz & C Eng. Lyon: IARC Press.

You MJ, Castrillon DH, Bastian BC, O'Hagan RC, Bosenberg MW, Parsons R, Chin L & DePinho RA 2002 Genetic analysis of Pten and Ink4a/Arf interactions in the suppression of tumorigenesis in mice. *PNAS* **99** 1455–1460.